# Baro-INS Integration with Kalman Filter

Vivek Dadu[c],B.Venugopal Reddy[a], Brajnish Sitara[a], R.S.Chandrasekhar[a] &
G.Satheesh Reddy[a*]

[c]Hindustan Aeronautics Ltd, Korwa, India.
[a]Research Centre Imarat, India.

## ABSTRACT

Conventionally a third order vertical channel damping loop is employed to reduce the errors due to accelerometer bias and prevent the divergence of vertical channel. In this study, a feed back kalman filter is adopted to fuse measurements from baro altimeter with that of INS. It will be shown through simulation results, that such a filter effectively damps the growth of vertical error.

**Keywords:** INS, Baro integration, Kalman Filter, Navigation

## 1. INTRODUCTION

Inertial Navigation Systems(INS) are ubiquitiously employed to provide position and velocity information. However, navigation information from INS gets degraded over time as INS errors are nonlinear and accumulate over time. The errors can be divided as horizontal errors and error in vertical channel. Error in the vertical channel directly contributes to error in altitude estimate. Due to Schuler damping, the horizontal errors are bounded and oscillate with a frequency equal to 0.00124 rad/s, known as the Schuler frequency. Due to undamped vertical channel, the errors in the vertical channel are not bounded and hence, while the latitude and longitude estimates from an INS are within the limits, the altitude estimate could have large deviation from true value.

Measurements from other external sources are used in conjunction with the INS measurements, to keep the error growth in the vertical channel within bounds. In this article, altitude measurements from the baro-altimeter and the INS measurements are fused with a Kalman filter to obtain an accurate estimate of the flight altitude.

The horizontal errors are corrected with a INS-GPS Kalman filter fusion scheme. However, due to the relatively poor VDOP as compared with HDOP, the altitude reference provided by the GPS is inferior to the Baro-altimeter/Radio-altimeter indicated height. Hence Baro-Inertial integration.

### 1.1 Divergence of vertical channel

Let us examine the error growth in altitude due to error in the estimate of computed gravity. Computed gravity using WGS-84 model is used to compensate for the actual gravity in the INS navigation. However, the WGS-84 computed gravity cannot always account for the several nonlinearities like the altitude variations, position influenced centrifugal acceleration that affect the actual sensed gravity. In the following, the treatment given in[3] is followed to explain the instability in altitude computation.

The accelerometer measured force is given by

$$A = \ddot{Z} + g$$

where $Z$ is the displacement and the $g$ is the gravity compensation.

$$g = g_0 \left(\frac{Z_0}{Z}\right)^2$$

* E-mail: sat_rins@yahoo.com, Telephone:(+91) 40-24306124, Fax: (+91) 40-24306626

Let $Z = Z_0 + h$, then

$$g = g_0 \left(1 + \frac{h}{Z_0}\right)^{-2}$$

$g_0$ is the value for gravity at $Z_0$ and $g$ is the value at $Z$.

Using Taylor series expansion,

$$\begin{aligned} g &= g_0 \left(1 - \tfrac{2h}{Z_0} + \cdots\right) \\ g &\cong g_0 - \left(\tfrac{2g_0}{Z_0}\right) h \end{aligned}$$

Thus,

$$\begin{aligned} A &= \ddot{Z} + g \\ \Rightarrow \quad A &= \ddot{Z} + g_0 - \left(\tfrac{2g_0}{Z_0}\right) h \end{aligned}$$

Since $Z = Z_0 + h$, $\ddot{Z} = \ddot{h}$.

$$\ddot{h} - \left(\frac{2g_0}{Z_0}\right) h = A - g_0$$

Due to error in the measurement of specific force, usually caused due to error in g-modelling, the error in the altitude is obtained by following equation

$$\Delta\ddot{h} - \left(\frac{2g_0}{Z_0}\right) \Delta h = \Delta A \tag{1}$$

Taking laplace transform of eqn.1 yields,

$$\begin{aligned} s^2\, h(s) - \left(\tfrac{2g_0}{Z_0}\right) h(s) &= \tfrac{\Delta A}{s} \\ h(s)\left[s^2 - \tfrac{2g_0}{Z_0}\right] &= \tfrac{\Delta A}{s} \\ \tfrac{h(s)}{\Delta A} &= \tfrac{1}{s\left(s^2 - \frac{2g_0}{Z_0}\right)} \end{aligned}$$

The characteristic equation is given by

$$s\left(s^2 - \frac{2g_0}{Z_0}\right) = 0$$

The characteristic equation has a positive pole/root at
$s = \sqrt{\frac{2g_0}{Z_0}}$, due to the negative term $\left(\frac{2g_0}{Z_0}\right) \Delta h$ on the LHS of eqn.1. The time domain solution of the differential equation is given by[3]

$$\Delta h = \frac{Z_0}{Z} \left(\frac{\Delta A}{g_0}\right) \left[cosh\sqrt{\frac{2g_0}{Z_0}}t - 1\right]$$

It may be observed that the error in altitude involves an exponential function *cosh* in its solution. Hence, the altitude error builds up exponentially in time. A $10\mu g$ error in the compensated specific force would result in a altitude error in excess of 2.5km over a two hour period.[2]

### 1.2 State diagram of the INS vertical channel

Fig.1 shows the state diagram for the vertical channel error given in eqn.1. $w(t)$ is the random noise in the specific force measurement. The positive feedback loop, $\frac{2g}{R_0}$ is the cause for instability of the vertical channel.

## 2. BARO-ALTIMETER

Baro-altimeters are invariably employed in every aircraft for pressure and altitude sensing. A baro-altimeter relying on atmospheric pressure, provides an indirect measure of height above a nominal sea level with an accuracy of 0.1%. As supplementary navigation aids, baro-altimeter measurements readily complement the INS altitude measurements, thereby restricting the growth of errors in the vertical channel of the INS.

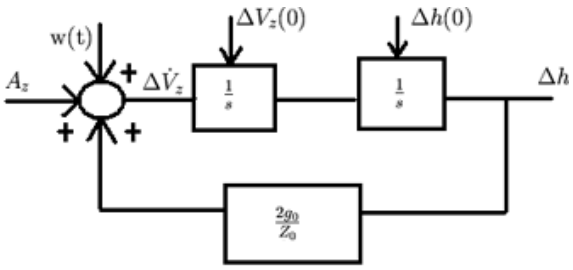


Figure 1. State Diagram of the INS vertical channel

### 2.1 Baro error model

The baro error is observed from the recorded empirical flight data. The autocorrelation plot of the baro error is shown in fig.2. From fig.2, it is clear the Baro error exhibits periodic behavior. The autocorrelation function for the plot shown in fig.2 is given by[8]

$$\phi(\tau) \quad = \sigma^2 e^{-\beta|\tau|} cos(\omega\tau) \tag{2}$$

and the values of parameters $\sigma^2$, $\beta$ and $\omega$ are derived from the empirical autocorrelation. In the particular case, the values of $\beta$ and $\omega$ have been worked out to be 0.04 and 0.17 respectively. The reconstructed autocorrelation plot using these values is given in fig.3. It is observed that the fitted autocorrelation function in fig.3 closely approximates the actual error autocorrelation function in fig.2. Two state variables are necessary to represent a random variable with such autocorrelation function.[8] One pair of quantities which provides this relation obeys the following differential equaitons[9]

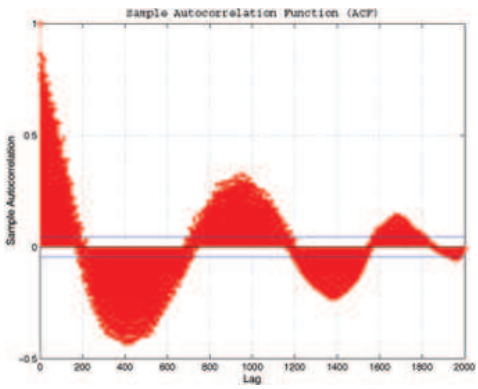


Figure 2. Error Autocorrelation of Baro Altimeter Data

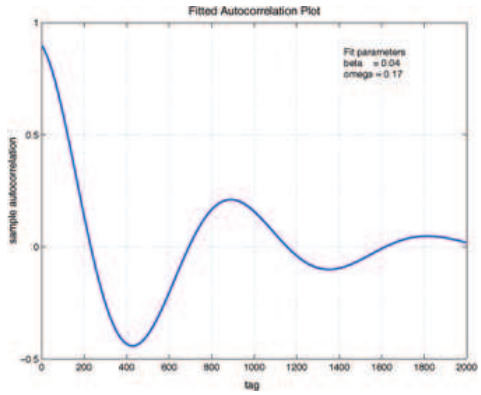


Figure 3. Autocorrelation plot with $\beta = 0.04$ and $\omega = 0.17$

$$\begin{aligned} \dot{x_1} \quad &= x_2 \ + \ w \\ \dot{x_2} \quad &= -\alpha^2 x_1 \ - \ 2\beta x_2 + (\alpha - 2\beta)w \end{aligned} \tag{3}$$

where

$$\alpha \quad = (\beta^2 + \omega^2)^{1/2}$$

The spectral density of the white noise w is $2\beta\sigma^2\delta(\tau)$.

The state diagram for the second order Gauss Markov process is given in figure 4. The state dynamics in the standard form is written down in eqn.4.

$$\begin{bmatrix} \dot{x_1} \\ \dot{x_2} \end{bmatrix} = \begin{bmatrix} 0 & 1 \\ -\alpha^2 & -2\beta \end{bmatrix} \begin{bmatrix} x_1 \\ x_2 \end{bmatrix} + \begin{bmatrix} 1 \\ \alpha - 2\beta \end{bmatrix} w \tag{4}$$

## 3. BARO INERTIAL LOOP

This section builds the necessary infrastructure as required for design of a Kalman filter for optimal mixing of Baro-altitude data with Inertial height data. In the INS navigation equations, the double pole at the origin in the $s$ plane means the mean square response to the white noise will grow without bound in the vertical channel. On the other hand the markov model for the baro altitude would keep the baro-altimeter error bounded. The following sections give the state transition model and the measurement model for estimating the error in INS altitude and Baro altitude measurements. The estimated error in INS altitude is fedback in closed loop configuration thereby restricting the growth of INS error in the vertical channel. The schematic of Baro-Inertial closed loop mixing is shown in fig.5.

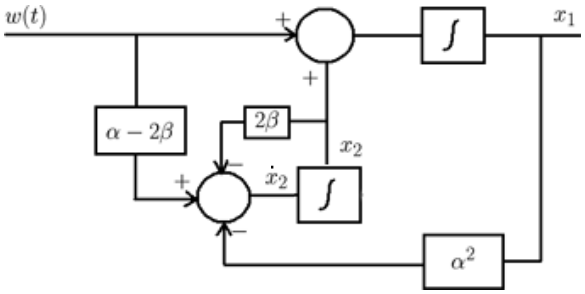


Figure 4. State diagram for $2^{nd}$ order Gauss Markov Process

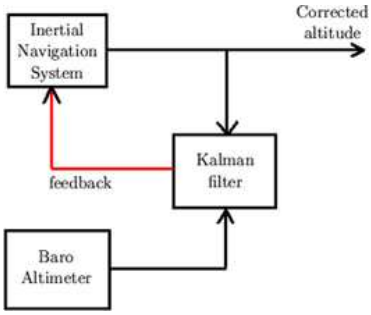


Figure 5. Baro Inertial Mixing Loop

### 3.1 State Model

$$\begin{aligned} \dot{\delta h_{ins}} &= \delta v_{dins} \\ \dot{\delta v_{dins}} &= w_{acc}(t) \\ \dot{\delta h_{baro}} &= \delta \tilde{h}_{baro} + w_{baro}(t) \\ \dot{\delta \tilde{h}_{baro}} &= -\alpha^2 \delta h_{baro} - 2\beta \delta \tilde{h}_{baro} + (\alpha - 2\beta) w_{baro}(t) \end{aligned}$$

In standard state space notation -

$$\begin{bmatrix} \delta h_{ins} \\ \delta v_{dins} \\ \delta h_{baro} \\ \delta \tilde{h}_{baro} \end{bmatrix}_{k+1} = \begin{bmatrix} 1 & \delta t & 0 & 0 \\ 0 & 1 & 0 & 0 \\ 0 & 0 & 1 & \delta t \\ 0 & 0 & -\alpha^2 \delta t & -2\beta \delta t \end{bmatrix} \begin{bmatrix} h_{ins} \\ v_{dins} \\ h_{baro} \\ \tilde{h}_{baro} \end{bmatrix}_k + \begin{bmatrix} 0 \\ w_{acc} \\ w_{baro} \\ w_{baro} \end{bmatrix}$$

$$X_{k+1} = \Phi_k \, X_k \, + \, W$$

#### 3.1.1 Process noise

$$Q = E\left[WW^T\right] \qquad W \triangleq [0, \; w_{acc}, \; w_{baro}, \; w_{baro}]^T$$

$$Q_k \approx \begin{bmatrix} A\,\frac{\delta t^3}{3} & A\,\frac{\delta t^2}{2} & 0 & 0 \\ A\,\frac{\delta t^2}{2} & A\,\delta t & 0 & 0 \\ 0 & 0 & 2\beta\sigma^2\delta t & 0 \\ 0 & 0 & 0 & (\alpha - 2\beta)^2 2\beta\sigma^2\delta t \end{bmatrix}$$

where $A$ is the power spectral density of the accelerometer and $\alpha$, $\beta$ and $\sigma^2$ are the parameters of the baro-error as given in the Baro error model.

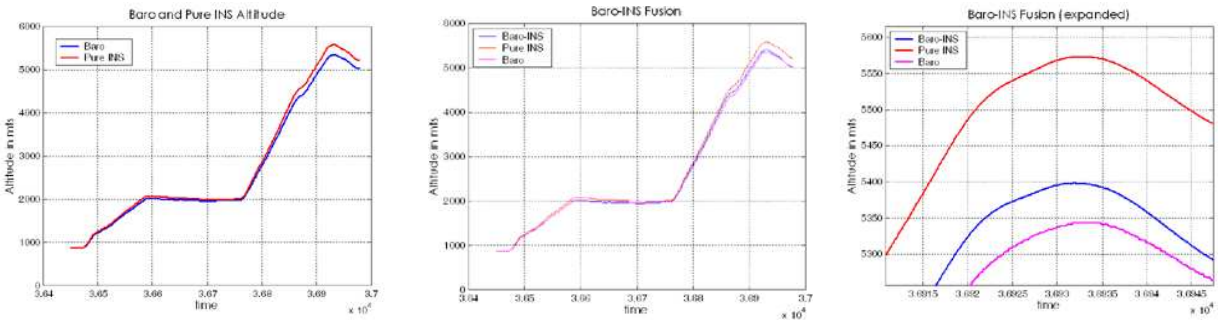


(a) Baro,INS (b) Baro,INS,Baro-INS (c) Magnified version of fig.6(b)

Figure 6. Pure and Hybrid Trajectory

### 3.2 Measurement model

The measurement is the difference between INS altitude and baro altitude.

$$\begin{aligned} Z &= h_{ins} - h_{baro} \\ &= (h_{true} + \delta h_{ins}) - (h_{true} + \delta h_{baro} + v_k) \\ &= \begin{bmatrix} 1 & 0 & -1 & 0 \end{bmatrix} \begin{bmatrix} \delta h_{ins} \\ \delta v_{dins} \\ \delta h_{baro} \\ \delta \tilde{h}_{baro} \end{bmatrix} + v_k \end{aligned}$$

#### 3.2.1 Measurement noise

$$R = E\left[v_k \; v_k^T\right]$$

The standard deviation in baro-altimeter error is taken as 10mts.

### 3.3 Kalman filter

The usual Kalman filter equations are given by

#### 3.3.1 Prediction step

$$\begin{aligned} X_{k+1/k} &= \Phi_k \; X_{k/k} \\ P_{k+1/k} &= \Phi_k \; P_{k/k} \; \Phi_k^T + Q_k \end{aligned}$$

#### 3.3.2 Measurement update

$$\begin{aligned} K_{k+1} &= P_{k+1/k} \; H_k^T \left[H_k P_{k+1/k} H_k^T + R_k\right]^{-1} \\ X_{k+1/k+1} &= X_{k+1/k} - K_{k+1} \left[H_k \; X_{k+1/k} - Z\right] \\ P_{k+1/k+1} &= P_{k+1/k} - K_{k+1} \; H_k \; P_{k+1/k} \end{aligned}$$

with usual notation followed in literature for Kalman filter.

## 4. RESULTS

The Pure INS and Baro indicated altitude profiles are obtained in the single flight operation. The profiles to be fused are indicated in fig.6(a). To exemplify the performance of the filter, the picture shown in fig.6(b) is magnified as shown in fig.6(c). It can be seen from the magnified version, that the Baro-INS integrated altitude error is around 30-50 mts and the INS error is corrected upto 150-200 mts at the maximum.

### 4.1 Evidence of convergence of the filter

#### 4.1.1 Error Covariance Matrix

The fig.7 shows the exponential convergence of the diagnol elements of the error covariance matrix of the filter.

#### 4.1.2 Filter Gain

The stabilization of filter gain is shown in fig.8

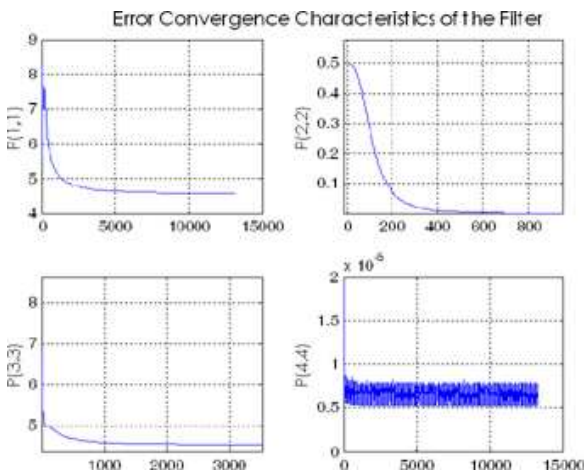


Figure 7. Diagnol elements of the Error Covariance Matrix

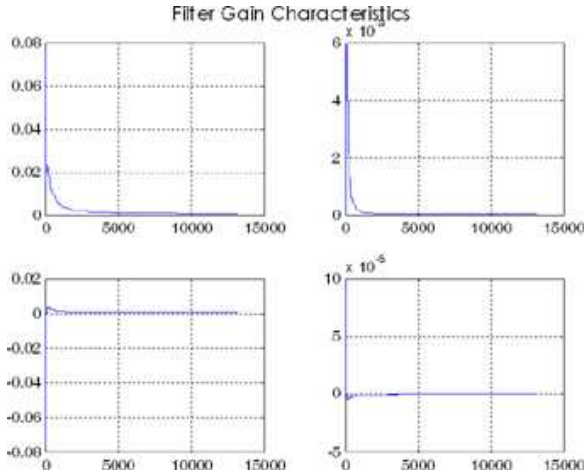


Figure 8. Filter Gains

## 5. CONCLUSION

A suitable kalman Filter is designed for fusing the measurements from baro-altimeter and INS navigation output.The filter output is feedback to INS system in a tightly coupled integration.The performance of filter is analyzed and found to be well behaved in the presence of varying noise levels.This adaptive feature of the filter is highly desirable in the design of integrated navigation systems.Though the paper presents vertical damping with help of Baro-Altimeter, the same design could be employed to damp the INS vertical channel with non dead-reckoning altitude measurements from other systems like GPS, Doppler et cetra.

## REFERENCES


1. I Y Bar-Itzhack, N Berman **Control Theoretic Approach to Inertial Navigation Systems**, *J. Guidance*, Vol. 11, No. 3, May-June 1988.
2. D H Titterton, J L Weston **Strapdown inertial navigation technology**, *IEE*, London, 1997.
3. G M Siouris **Aerospace Avionics System : A Modern Synthesis**, *Academic Press*, NewYork.
4. J H Kim, S Sukkareieh **A baro-altimeter augmented INS/GPS navigation system for uninhabited aerial vehicle** *SatNav 2003*, 22-25 July 2003, Melbourne, Australia.
5. William S. Windall, Prasun K. Sinha **Optimizing the Gains of the Baro-Inertial Vertical Channel** *AIAA J. Guidance and Control*, Vol.3, No.2, Mar-Apr 1980.
6. Brown, R.G., Hwang, P.Y.C. **Introduction to Random Signals and Applied Kalman Filtering**, John Wiley, 1997.
7. P.M.Barham, P.Manville, **Application of Kalman Filtering to Baro/Inertial Height Systems**, *Theory and Applications of Kalman Filtering*, CT Leondes (Ed.), NATO Agardograph 139, 1970.
8. S.Vathsal, **Design and Simulation of Closed Loop Ground Alignment of Inertial Platforms with Sway Motion**, *AIAA Journal of Guidance*, Vol. 9, May-June 1986.
9. Arthur Gelb, **Applied Optimal Estimation**, The M.I.T. Press, Cambridge.